Colloids and Surfaces A: Physicochem. Eng. Aspects 486 (2015) 161–171

Contents lists available at ScienceDirect

Colloids and Surfaces A: Physicochemical and Engineering Aspects

journal homepage: www.elsevier.com/locate/colsurfa

Preparation of protein nanoparticle by dynamic aggregation and ionizing-induced crosslinking

E. Achilli[a,1], G. Casajus[a,1], M. Siri[b], C. Flores[a], S. Kadłubowski[c], S. del V. Alonso[b], Mariano Grasselli[a,*]

[a] Laboratorio de Materiales Biotecnológicos (LaMaBio), Universidad Nacional de Quilmes-IMBICE (CONICET-CICPBA), Bernal, Argentina
[b] Laboratorio de BioMembranas (LBM), Dpto. de Ciencia y Tecnología, Universidad Nacional de Quilmes-IMBICE (CONICET-CICPBA), Bernal, Buenos Aires, Argentina
[c] Institute of Applied Radiation Chemistry, Lodz University of Technology, Wroblewskiego 15, 93-590 Lodz, Poland

HIGHLIGHTS

- Albumin nanoparticles can be prepared by ionizing radiation (gamma rays or electron beam).
- Protein dynamic aggregation depends on ethanol concentration.
- Ionizing radiation stabilizes albumin nanoparticles.
- Albumin nanoparticles do not lose protein structure-function.
- Protein nanoparticles can be prepared from a mixture with albumin.

GRAPHICAL ABSTRACT

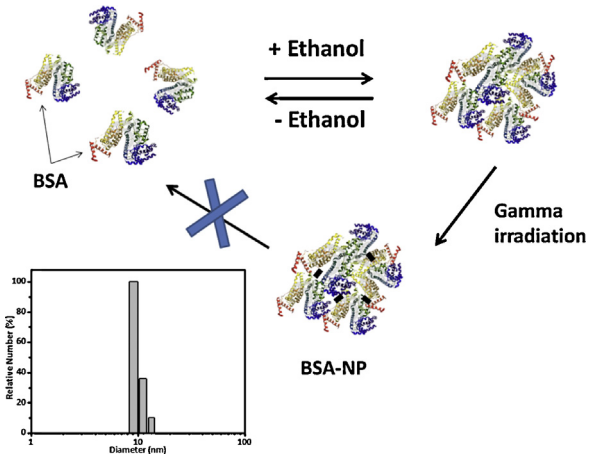

ARTICLE INFO

Article history:
Received 6 June 2015
Received in revised form 8 September 2015
Accepted 16 September 2015
Available online 21 September 2015

Keywords:
BSA nanoparticles
Dynamic protein aggregation
Electron beam irradiation
Lysozyme/BSA nanoparticles

ABSTRACT

Globular proteins can be considered as nanotools useful to perform a variety of chemical reactions. These biological macromolecules have very complex and detailed topological characteristics responsible for their several functions, which can be used for technological applications.

Albumin is one of the few commercially available proteins with potential use in the preparation of nanomaterials by the bottom-up strategy. Albumin nanoparticles (NPs) can be prepared by several methods, but the preservation of the structure of the native protein in the final structure has not yet received too much attention.

Our research group has recently reported the use of ionizing radiation to obtain albumin NPs. The irradiation of an ethanol solution of bovine serum albumin (BSA) allows obtaining protein NPs in the size range of 20–40 nm. However, a plausible mechanism to explain the process of preparation of protein-based NPs has not yet been described. In this work, we performed a series of experiments to prepare protein based NPs in two independent steps: (i) dynamic aggregation of BSA by ethanol and (ii) radiation-induced cross-linking by gamma or electron beam irradiation. Dynamic light scattering (DLS), circular dichroism (CD), Fourier Transform Infrared Spectroscopy (FT-IR) and UV spectroscopy measurements provided

* Corresponding author at: LaMaBio, Depto. de Ciencia y Tecnología, Universidad Nacional de Quilmes, Roque Sáenz Peña 352 (B1876BXD) Bernal, Argentina. Fax: +54 11 4365 7132.
E-mail address: mariano.grasselli@unq.edu.ar (M. Grasselli).
[1] Both authors contributed equally to this study.

http://dx.doi.org/10.1016/j.colsurfa.2015.09.047

additional information about the conformation of BSA. No spectroscopy signal changes of aromatic amino acids were detected by UV and a loss of 20% of the alpha helix secondary structure was determined by CD. Drug-carrier functions were studied by binding and releasing assays of Merocyanine 540. BSA-NPs showed a drug-carrier behavior similar to that of BSA. Finally, we evaluated the possibility to prepare protein NPs containing more than one protein using the same procedure. Bi-protein NPs were prepared from lysozyme and BSA. The bi-protein NP showed enzymatic activity of lysozyme, which confirms the functionality of the NP prepared by this novel method.

1. Introduction

From the technological point of view, globular proteins can be considered as nanotools useful to perform a variety of chemical reactions, such as hydrolysis of different molecules, catalysis of oxidation or reduction processes. These biological macromolecules have very complex and detailed topological characteristics responsible for their several functions.

Preparation of nanomaterials from proteins by the bottom-up strategy is difficult as a consequence of the reduced availability of these materials. However, commercially available proteins obtained from natural or recombinant sources, such as gelatin, collagen, albumin or papain, can be used as starting building blocks to prepare nanomaterials. In addition, proteins represent excellent raw materials considering biological applications because they have advantages such as absorbability and low toxicity of the degradation end products [1,2].

Serum albumin is the most abundant plasma protein in the blood of mammals. It is also one of the longest known and probably the most studied of all proteins [3,4]. Its numerous functions have attracted the interest of scientists and physicians for generations [5]. Albumin in its native monomeric form is a commercial product with many laboratory and industrial applications. *In vitro* applications include its use as medium component for cell culture, cryopreservation and stem cell expansion [6]. In these applications, albumin works as a natural carrier to deliver important nutrients to cells, and binds toxins to avoid toxic effects and excessive amounts of proteins such as hormones and growth peptides, acting as slow-release agent to keep these substances stable. Also, the coagulation properties of albumin allow its use in many implantable biomaterials, surgical adhesives and surgical sealants [7]. Elzoghby et al. have recently reviewed several *in vitro* and *in vivo* studies performed with albumin NPs in which these NPs showed exciting results about the controlled delivery of therapeutic agents, high drug loading capacity in combination with biodegradability, biocompatibility and the possibility of covalent link of drug targeting ligands [8]. Albumin NPs can be prepared by several methods. Three of these methods involve classical protocols such as desolvation, emulsification and thermal gelation [9]. Novel approaches such as nano-spray drying [10], nab-technology [11,12] and self-assembly [13,14] have also been reported. To improve the stability of NPs and avoid particle dissolution, chemical crosslinking with glutaraldehyde or heat denaturation are standard stabilization steps. However, the use of chemical agents may lead to toxic or undesirable reactions if the compound is not properly removed and the thermal process involves protein denaturation [15].

Our research group has recently reported the use of ionizing radiation to obtain albumin NPs [16]. The irradiation of an ethanol solution of bovine serum albumin (BSA) allows obtaining reaches protein NPs in the size range of 20–40 nm. This method has also been successfully applied to prepare NPs from papain [17].

So far, no data have been published to explain the role of additives/radiation in the mechanism of protein-based NP formation. The aim of this work was to prepare protein-based NPs with maintained protein functionality by ionizing radiation, by a series of experiments in two independent steps. The first, by dynamic aggregation of BSA in ethanol and the second by radiation-induced cross-linking.

2. Materials and methods

Bovine serum albumin (BSA), Fraction V, was obtained from Sigma–Aldrich. Lysozyme (Hansozyme) was kindly donated by Chris-tian Hansen Argentina. All other reagents were of analytical grade and used as received. BSA was dissolved in phosphate buffer 30 mM pH 7. Different amounts of ethanol were added drop-wise onto the protein solution, keeping the temperature at 0 °C under constant stirring. BSA solutions were irradiated with gamma-rays from a ^{60}Co source (Planta de Irradiación Semi-Industrial, Centro Nacional de Energía Atómica Ezeiza, Argentina) at a dose rate of 1 kGy/h at 5–10 °C. After irradiation, protein solutions were diluted to a suitable concentration with phosphate buffer saline (PBS) for further experiments.

Electron beam irradiation was performed by short pulses of fast electrons [pulse duration: 4 μs, pulse frequency: 20 Hz, electron energy: 6 MeV, absorbed dose of ionizing radiation per shot (irradiation times: 6 s): 1 kGy generated by an ELU-6 linear accelerator (Eksma, Russia)].

Particle size was determined by dynamic light scattering (DLS) at 25 °C using a 90Plus/Bi-MAS particle size analyzer, with a light source of 632.8 nm and a 10 mW laser. Each result is the average of three measurements. Samples were kept at 4 °C until analyzed, and measurements were carried out on days 1 and 30 after sample preparation.

Circular Dichroism (CD) measurements were carried out at 20 °C on a Jasco 810 spectropolarimeter equipped with a Peltier-effect device for temperature control (Jasco Corporation, Japan). Six or ten spectra were recorded and averaged.

Functionality assays were carried out with the fluorescent probe Merocyanine 540 (MC540) to test binding affinity and kinetic release profile at room temperature. The encapsulated drug was separated from the free drug with a Vivaspin 500, 3 kDA MWCO, GE Healthcare tubes, by centrifuging samples at different times in an Eppendorf Centrifuge 5804 R at 12,000 rpm, 4 °C for 20 min (each experimental datum corresponds to triplicate determinations). For the kinetic release profile assay, the methodology was similar: aliquots of the samples were taken at selected times. Samples were measured by UV–vis spectroscopy using a Nano-drop 1000 spectrophotometer (Thermo Scientific). Data were analyzed using GraphPrad Prism 5.0 software and Michaelis–Menten model was fitted by non-linear regression analysis. FT-IR and fluorescence spectroscopy were performed to study the protein-probe interaction. FT-IR spectroscopy was analyzed using a multi-reflexion ATR module. About 500 μl of each sample was blow-dried on ZnSe crystal with 45° of inclination. The spectra were recorded with 64 scans and a 1 cm^{-1} resolution. Data were analyzed by IRSolution Software and then by GraphPad Prism 5.0 software. The fluorescence study was done using a S2 Scinco spectrofluorometer (Jasco). Samples

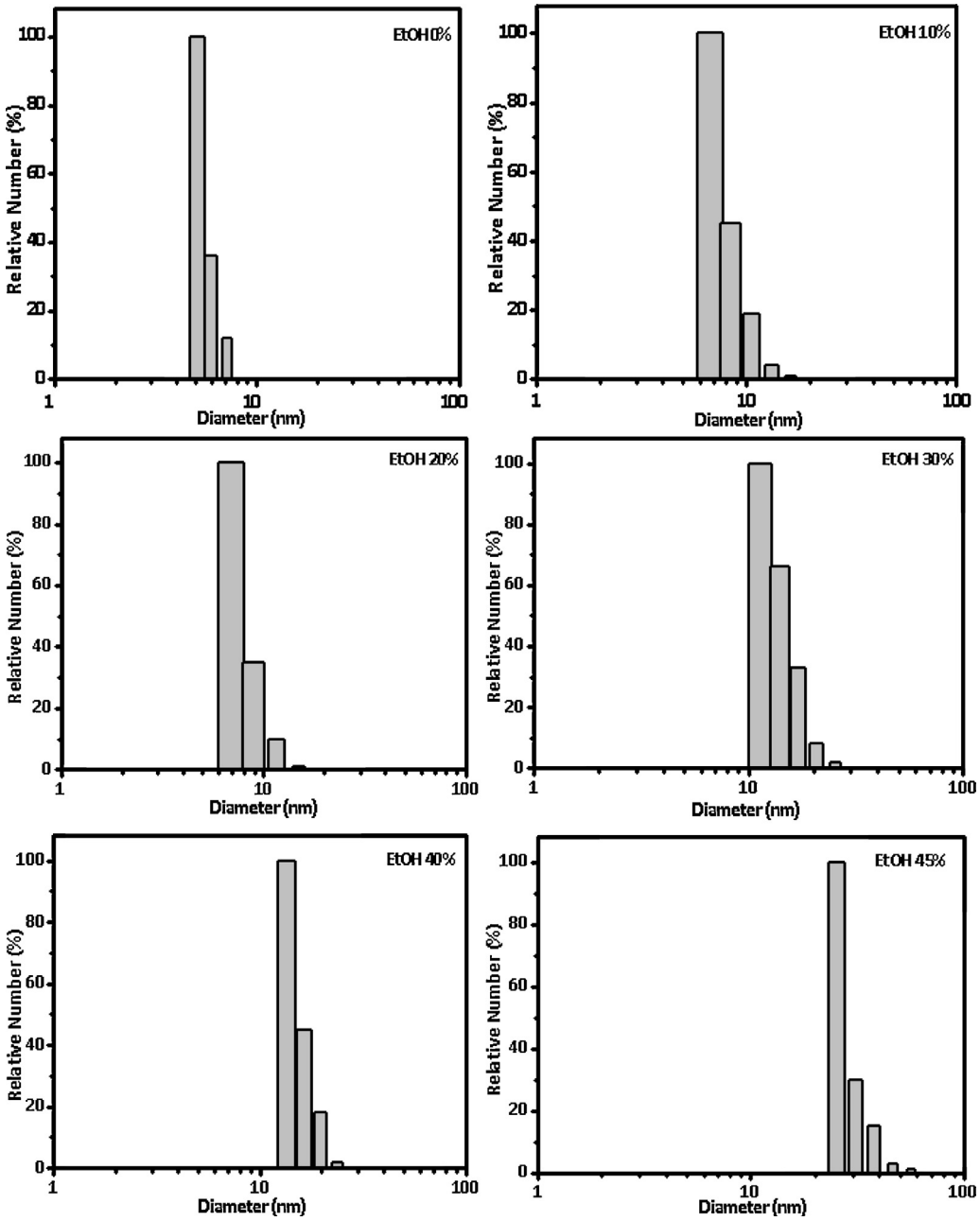

Fig. 1. Dynamic light scattering analysis. Plots of particle diameter distribution of BSA solutions containing different amounts of ethanol: (a) BSA in buffer solution; (b) with the addition of 10% v/v ethanol; (c) 20% v/v ethanol; (c) 30% v/v ethanol; (c) 40% v/v ethanol and (d) 45% v/v ethanol. All measurements correspond to the average of three measurements of 30 s.

were excited at 280 and 295 nm, while emission was set at 337 and 340 nm respectively. The GraphPad Prism 5.0 software was used to analyze the data collected. The calculation of the dissociation constant (K_d) and maximum drug binding (B_{max}) was determined by fitting the experimental data to Michaelis–Menten model as described in Sevilla et al. [18].

3. Results and discussion

3.1. NP preparation with BSA

Engineered NPs are attracting great interest for application in different biological fields. The high absorption efficiency to biological tissues of these nanosized materials constitutes one of the most relevant characteristics for cosmetic and medical applications [19–21].

For a long time now, albumin has attracted the attention of the pharmaceutical industry because it is the most abundant serum protein and has the ability to bind a wide variety of drug molecules and alter their pharmacokinetic parameters. Albumin NPs can be prepared by emulsification, but this method requires an organic solvent to remove the oil and surfactant. Another method commonly used to prepare protein NPs is the desolvation process with organic solvents [9,22]. However, the NPs obtained are not stable. To avoid particle dissolution, standard stabilization steps are chemical cross-linking with glutaraldehyde or heat denaturation, but it is also known that albumin oligomerization by thermal process involves the loss of its native structure [1].

Globular proteins are macromolecules which are very sensitive to the microenvironment. The addition of polar solvents or solutes to a protein solution, under controlled conditions, is able to precipitate globular proteins without loss of their native structure. In the case of BSA, more than 40% ethanol is required to induce its precipitation [23].

As previously reported in Soto Espinoza et al., 2012, BSA-NPs can be prepared from irradiation of an ethanol solution of BSA at sub-precipitating concentrations. In the present study, we first analyzed the influence of ethanol on protein samples before the irradiation process. Fig.1 shows the diameter distributions of a BSA solution as a function of ethanol concentration. It is important to remark that the solvent was added at temperatures between 0 and 5 °C to avoid protein denaturation. Thereafter, samples were diluted in the corresponding ethanol-buffer mixture to fit the DLS measurement conditions. The histogram shows that BSA aggregation occurred with only 10% of ethanol added to the protein solution. These aggregates showed slight increases in size in the range of 5–45% of ethanol (v/v) in the protein solution. Fig. 2 shows the DLS data compiled in a plot of hydrodynamic diameter versus ethanol percentage of the protein solution. Particles two-fold larger than the BSA hydrodynamic diameter were found at around 40% ethanol. Beyond this ethanol concentration, a sharp increase in the particle diameter was observed (c.a. 30 nm at 45% ethanol). NPs diameter could not be measured of BSA solutions at higher ethanol concentrations because of the increase in viscosity and/or physical gel formation [24].

Dilution of the ethanol–protein samples with water (more than ten-fold) reduced the ethanol concentration, with the concomitant disappearance of aggregates. Only the BSA molecule signal was found in the DLS histogram (data not shown). Meanwhile, the dilution with the same ethanol–water ratio showed no size distribution changes in the DLS histogram. This phenomenon is compatible with a completely reversible aggregation process at sub-precipitating ethanol concentrations. Therefore, DLS measurements of water-diluted BSA samples are a straightforward test of the stability of protein NPs.

In the following step, we analyzed the particle size distribution of ^{60}Co gamma ray-irradiated samples. It has been previously demonstrated that irradiated aqueous BSA solution does not reach an appreciable change in the particle size up to a dose of 20 kGy [16]. The distribution of hydrodynamic diameters of the ethanol solution of BSA (35% v/v) under non-irradiated and irradiated conditions is shown in Fig. 3. An almost similar particle size distribution is found after irradiation, which means that the process itself does not induce aggregation of protein molecules. BSA-NP samples proved to be stable even after dilution. Fig. 4 shows a summary of the changes in the mean sizes of particles at different experimental conditions, considering presence/absence of ethanol and irradiated/non-irradiated conditions.

BSA molecules are mainly in a monomeric form in water/buffer solutions. Therefore, the aggregation process is not favorable under these conditions. The addition of ethanol shifts the equilibrium to the protein aggregation (which it has a solvent dependence, as it is shown in Fig. 1). After crosslinking, this equilibrium is shifted to the aggregation condition, increasing the particle size. Changing the medium to an unfavorable aggregation condition (by dilution with buffer, or solvent exchange by Size Exclusion Chromatography), all non-covalent bounded BSA molecules will be detached from the NP, with the exception of the cross-linked ones.

Analysis of the data allowed inferring that the mechanism of BSA-NP formation is a combination of a dynamic aggregation and radiation cross-linking effect of BSA (Fig. 5). The main effect of the solvent is the reduction of the water shell around the protein and the reduction of the dielectric constant of the solution, which increases the electrostatic interaction between BSA molecules, inducing partial aggregation. Other polar water-soluble solvents, such as acetonitrile and isopropanol, are also able to form BSA-NPs, while other protein precipitants, such as ammonium sulfate or sodium chloride salts, are not able to induce the formation of BSA-NPs [16].

Table 1
Average of mean diameter of BSA-NPs in buffer after stabilization by gamma irradiation or chemical cross-linking. Both NPs were prepared in ethanol 35%.

Condition	Diameter (nm)	SD(nm)
Irradiation with 10 kGy dose	20.5	3.5
Glutaraldehyde 2.5%	17.5	3

In the following experiment, an ethanol BSA solution was saturated with different gases previous to irradiation. Different gas atmospheres during the irradiation process had a minor, but measurable, effect on the hydrodynamic diameter of the BSA-NPs. Fig. 6 shows the same ethanol BSA solution, saturated with air, nitrogen or acetylene before gamma irradiation with 10 kGy at a dose rate of 1 kGy/h (samples were prepared in triplicate). Therefore, radiation active gases, such as oxygen or acetylene, allowed obtaining NPs of larger sizes. This can occur through a complex free radical pathway, which can be altered by other additives in the cross-linking process induced by the ionizing radiation. Further studies are currently in progress.

Radiation-induced crosslinking is a well-known process to create new chemical bonds, which has been described for several synthetic and natural polymers dissolved in water and irradiated with gamma and/or electron beam [25–28]. The ability to induce macromolecular rearrangements of the molecules in solution, reaching a macro-hydrogel (mainly intermolecular cross-linking) or nano-gels (mainly by intramolecular cross-linking), can be tuned by changing the experimental conditions.

The gamma radiation-induced protein NP preparation carried out in the present study was done at low dose rate (1 kGy/h). To support a two-step mechanism (aggregation and cross-linking), a very short and a high-dose-rate irradiation was performed using pulsed electron beam. Oxygen-free (argon-saturated) samples were prepared to avoid other side reactions. This experiment was also used to determine the minimum irradiation dose required to prepare protein NPs under deoxygenated conditions. The electron beam accelerator was set to deliver a dose of 1 kGy per pulse (6 s). One and two pulses were performed onto degassed BSA samples. In the case of the 2 kGy irradiation condition, two experimental setups were investigated: (i) a continuous irradiation without delay between pulses (Fig. 7, 2 kGy) or (ii) a 300 s delay between pulses (Fig. 7, 1 + 1 kGy), to allow relaxation of the sample and avoid an increase in the local temperature. Fig. 7 shows the plot of the average hydrodynamic diameter of NPs in ethanol solution (35% v/v) of BSA-irradiated samples under these conditions. The 1 kGy dose shows a broad standard deviation which could be assigned to an incomplete cross-linking process, whereas the 2 kGy dose shows NP formation irrespective of the irradiation conditions. Higher irradiation doses also reached NP formation in a very homogeneous manner (data not shown).

This method based on radiation-induced intramolecular crosslinking was developed by Ulanski and Rosiak [29,30]. The main advantage of this method is that it can be carried out in a pure polymer/solvent system, free of any monomers, initiators, crosslinkers or any other additives, therefore it seems to be especially well suited for the synthesis of high-purity products for biomedical use. In this approach pure aqueous solution of a polymer is subjected to a short (a few microseconds), intense pulse of ionizing radiation. In this way, many radicals are generated simultaneously along each polymer chain, and their intramolecular recombination leads to the formation of nanogels. It has been shown that such a proce-

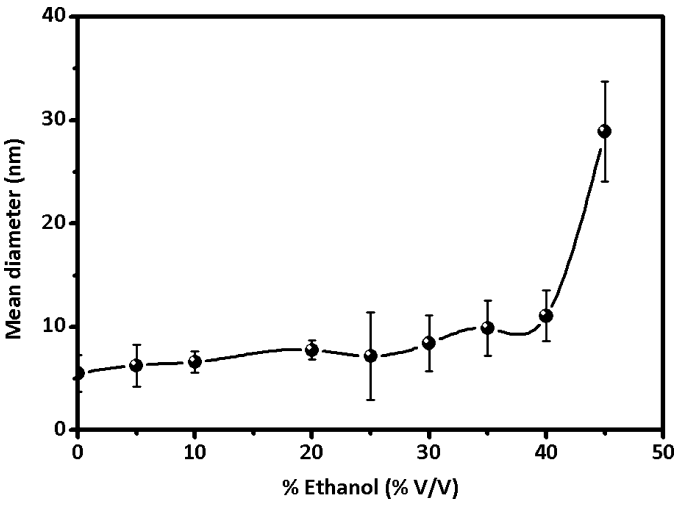

Fig. 2. Mean hydrodynamic diameter of BSA solution containing increasing amounts of ethanol.

dure can be used to synthesize nanogels from simple hydrophilic polymers, e.g., poly(vinyl alcohol) [29], poly(*N*-vinylpyrrolidone) [27,28,30–32], poly(vinyl methyl ether) [33] and poly(acrylic acid) [26,34].

The use of radiation to control the nanostructure of peptides and proteins was demonstrated by Furusawa et al. [34] and by Akiyama et al. [35] where nanometer-sized gelatin particles were produced. Recently, the synthesis of radio-induced nanoparticles using more complex structures such as enzymes (papain) was reported by Varca et al. [17]. In this case, bityrosine bond formation between tyrosines present in proteins has been proposed as a main mechanism for crosslinking inside the protein NPs [17].

To better characterize the protein NPs obtained, we next carried out spectroscopy analysis. UV–vis, CD and FT-IR spectroscopy are very well known techniques used to characterize proteins. These techniques are sensitive to detect instantaneous protein conformational changes. Our study focused on the formation and stability of protein NPs. We have previously demonstrated that near CD spec-

Table 2
Parameters (K_D and B_{max}) corresponding to fit BSA/MC450 and BSA-NP/MC450 to a Scatchard plot. Experimental data correspond to the measurements from Fig. 12.

$\lambda_{ex.}$ (nm)	Parameter	BSA/MC540	BSA-NP/MC540
295	B_{max}	2.1e-4 ± 1.0e-4	0.9e-4 ± 0.3e-4
	K_D	6.3e-4 ± 4.1e-4	2.8e-4 ± 1.3e-4
	R^2	0.97	0.95

R^2 is the correlation factor of the fitting process.

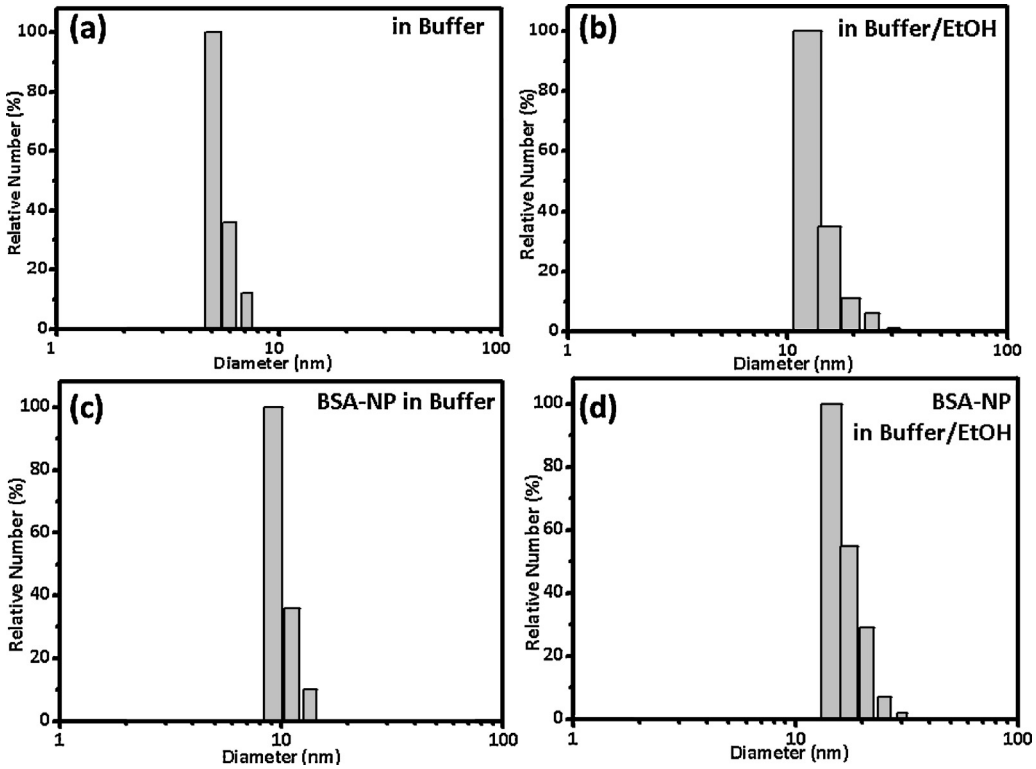

Fig. 3. Plots of particle diameter distribution of (a) BSA solution in buffer; (b) ethanol solution of BSA (35% v/v) under non-irradiated and (d) irradiated conditions (BSA-NPs). (c) BSA-NPs equilibrated in buffer solution.

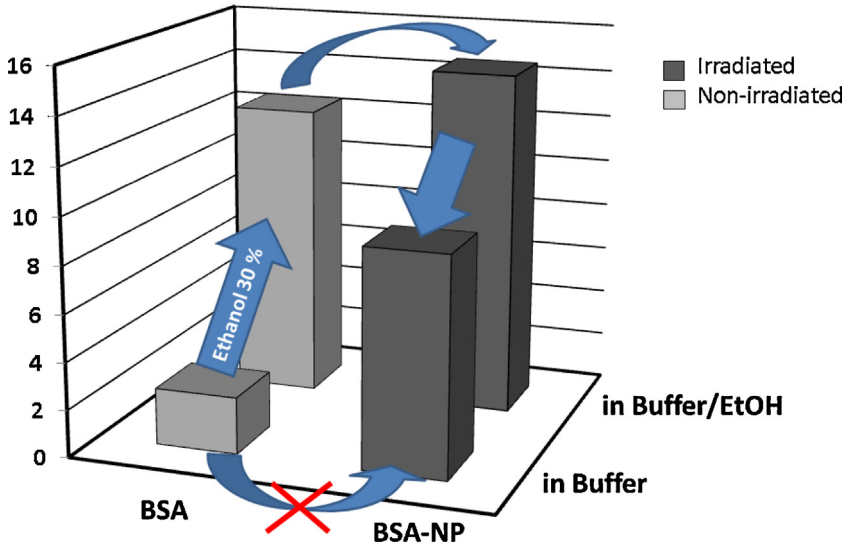

Fig. 4. 3D bar plot showing the evolution of the mean hydrodynamic diameter after the sequential procedure of protein NP preparation.

tral analysis of the irradiated samples shows no important changes in this 'fingerprint region' of aqueous samples of NPs. We attributed an increase in the CD signal of NP samples to a more rigid conformational structure of BSA [16]. In the present study, we performed CD spectroscopy onto BSA samples diluted in the same irradiation buffer containing ethanol. We compared the near CD spectra of the ethanol solution of BSA before and after irradiation (Fig. 8) and found no changes in the general 3D structure.

Considering the far CD spectra, secondary protein structure can be analyzed to find out complementary structural information. According to the UNIPROT data base, the three-dimensional structure of BSA (P02769—ALBU_BOVIN) has around 74% of alpha helix and 3% of beta-strand structures. Therefore, the total CD spectrum corresponds to the addition of signals from all structures, which is mainly the alpha helix signal shape (Fig. 9). The spectrum shows minimum peaks at 208 nm and 222 nm and a maximum at 192 nm. The addition of ethanol (35% v/v) showed no appreciable effect on the relative composition of the alpha helix, beta sheet and random structures. However, after irradiation (2 kGy), a reduction in the minimum peaks and in the maximum was detected (Fig. 9). These changes could be attributed to partial loss of secondary structures (alpha helix) and appearance of irregular structures. Random coil structures have very low CD signal contribution in the range of 210–240 nm and a negative signal in the range of 190–210 nm. Considering the height of the 208 nm peak, a reduction (loss) of 20% of the alpha helix secondary structure during the nano-structuring process can be estimated.

CD analysis gives a complete picture of all protein solutions but it is not possible to discriminate the presence of micro-heterogeneities; therefore, at least two possible scenarios can be expected: (i) some BSA molecules are completely denatured whereas others are completely unaltered, or (ii) all the BSA molecules are partially denatured.

Fourth-derivative analysis of UV–visible spectra (4dUVv) gives information mainly about aromatic amino acids. Alteration of the phenylalanine (Phe), tyrosine (Tyr) and tryptophan (Trp) microenvironments (polarity, hydration, hydrophobic interactions and packing density) can be followed by this technique. BSA has 27 Phe,

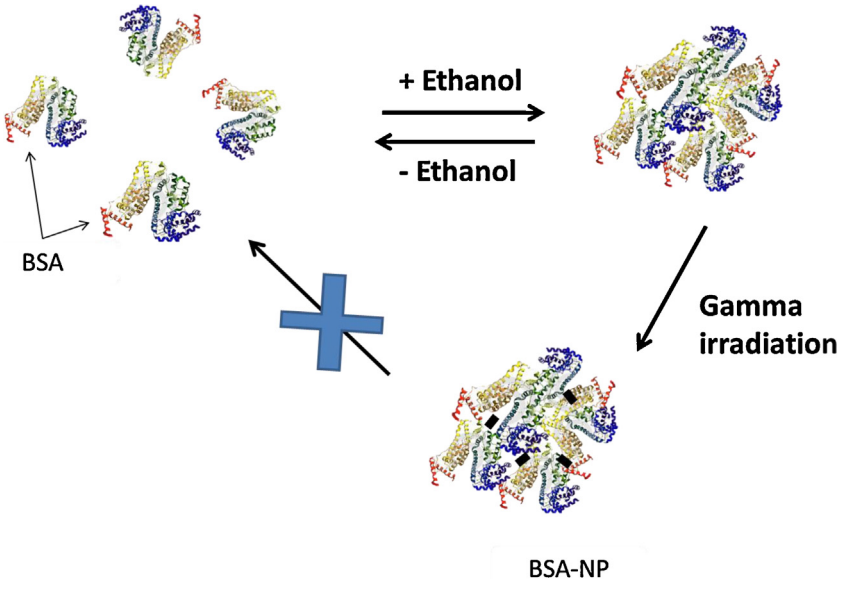

Fig. 5. Scheme of the proposed mechanism of formation of BSA-NPs by irradiation of an ethanol protein solution.

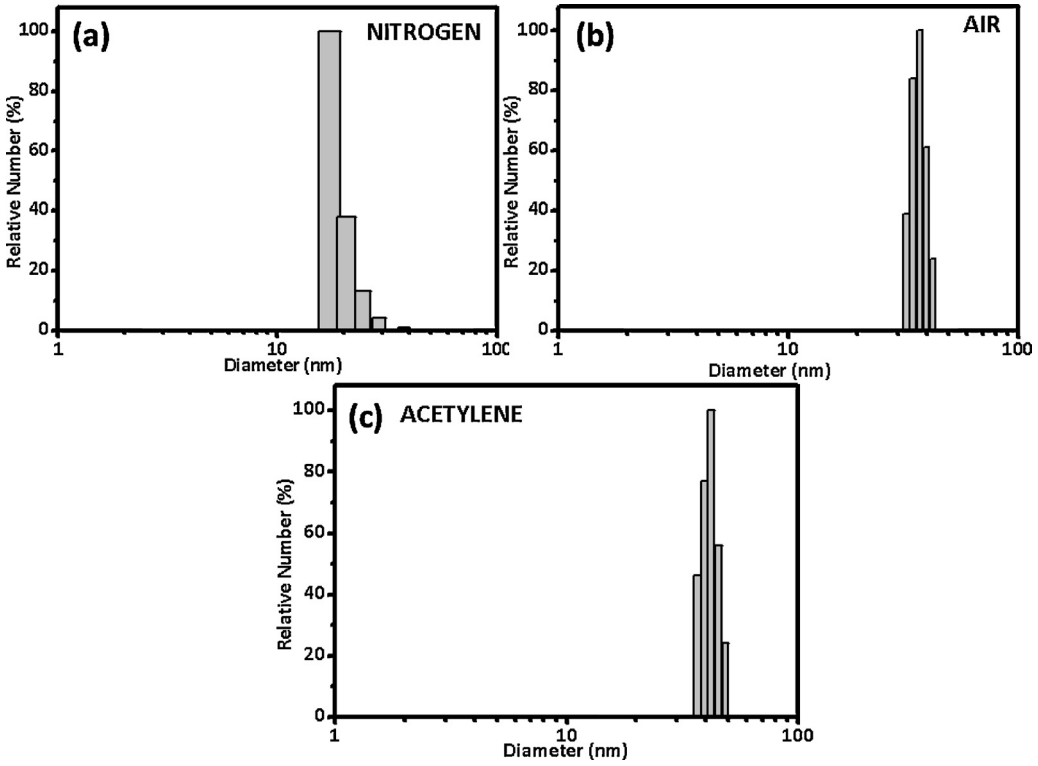

Fig. 6. Plots of particle diameter distribution of an ethanol solution of BSA (35% v/v) irradiated with 10 kGy in a gamma-ray chamber (a) under air atmosphere, (b) nitrogen-saturated sample and (c) acetylene-saturated sample. All measurements correspond to the average of three measurements of 30 s (samples were prepared in triplicate).

20 Tyr and only two Trp. The latter are located in domains I and II of the three BSA domains. BSA also has 35 cysteine residues, 34 of which are forming 17 disulfide bonds. These bridges have a weak absorption band in the UV region near 260 nm.

The 4dUVv spectra of the 2 kGy (1 + 1 condition) irradiated BSA samples had no absorbance peak shifts and the same spectral shape as the non-irradiated ones (Fig. 10), indicating that the microenvironment of aromatic amino acids keeps the same conformational features of the protein [16]. Only slight changes in the 250–260 nm range were noticed in the irradiated sample. According to the literature, this cannot be assigned to the aromatic amino acids. However, some modification of the sulphur-containing amino acids is possible. The spectrum corresponding to the 2 kGy-irradiated samples shows greater changes in this region (data not shown).

The CD and UV–vis data allow concluding that most of the BSA proteins in the samples kept their native structure. Thus, NPs should be formed by the aggregation of protein molecules with a minor random structure.

FT-IR analysis using the ATR module showed similar BSA and BSA-NP spectra in the amide regions (Fig. 11). Spectra are comparable to those of hydrated BSA samples prepared by other authors [36].

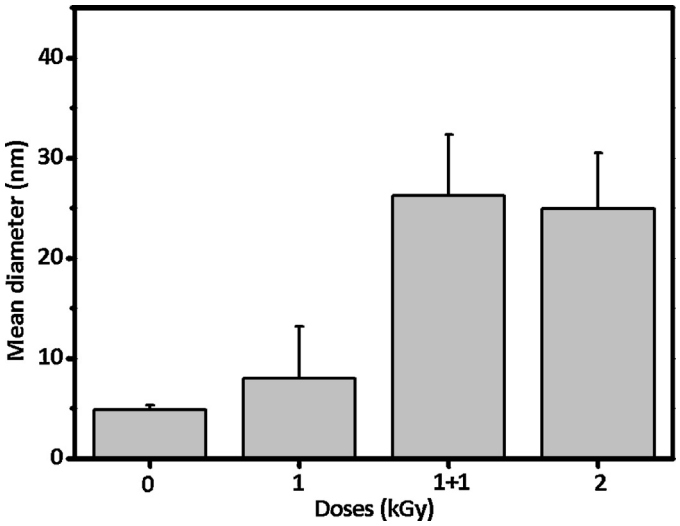

Fig. 7. Mean hydrodynamic diameter of an aqueous solution of BSA-NPs prepared by electron-beam irradiation at different doses. Condition 1 + 1 refers to a 2 kGy total dose delivery in two pulses with a delay of 300 s between them.

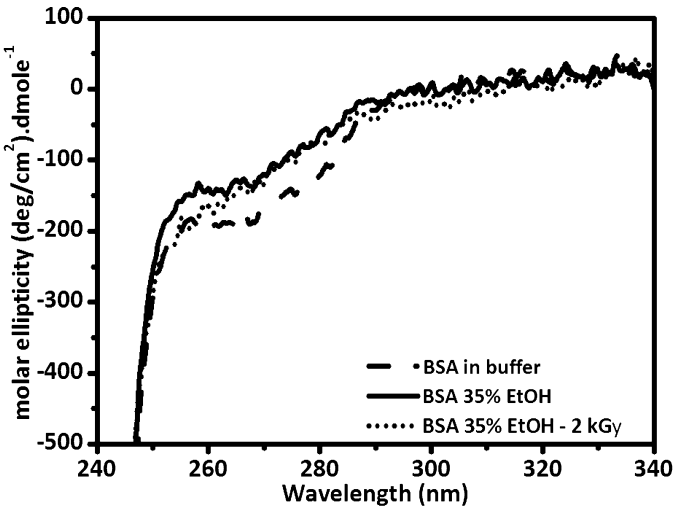

Fig. 8. Near CD spectra corresponding to BSA protein in (a) buffer solution, (b) with the addition of ethanol 35% v/v and (c) irradiated with the electron beam, 2 kGy (1 + 1 condition), in the presence of 35% v/v ethanol.

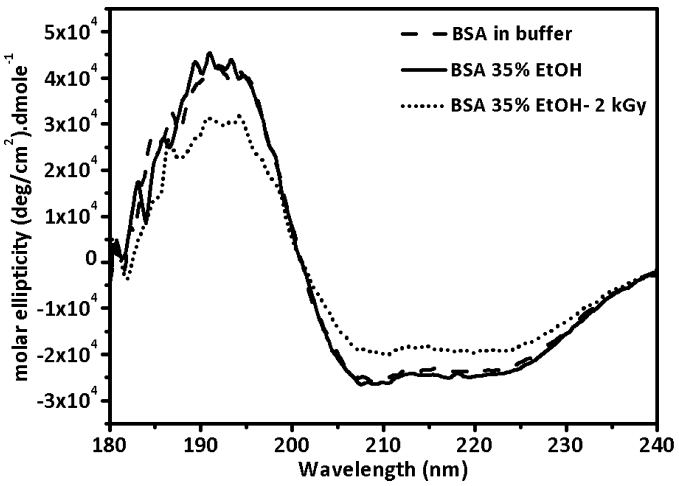

Fig. 9. Far CD spectra corresponding to BSA protein in (a) buffer solution, (b) with the addition of ethanol 35% v/v and (c) irradiated with the electron beam, 2 kGy (1 + 1 condition), in the presence of 35% v/v ethanol.

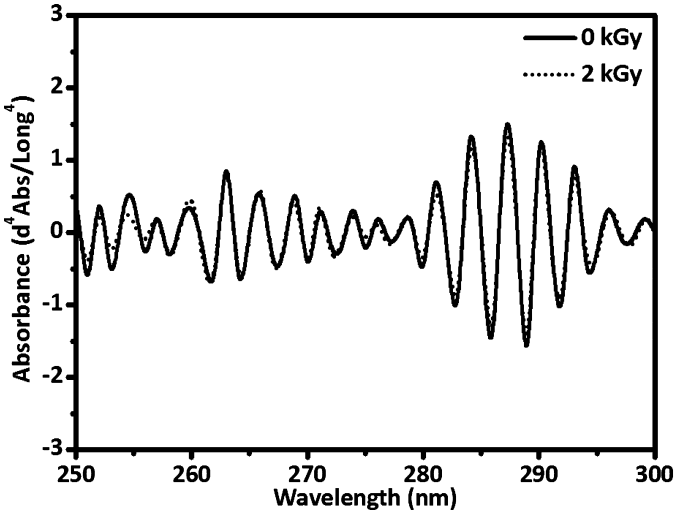

Fig. 10. Fourth derivative UV–vis spectra of BSA protein with the addition of ethanol 35% v/v irradiated with the electron beam at 2 kGy (1 + 1 condition).

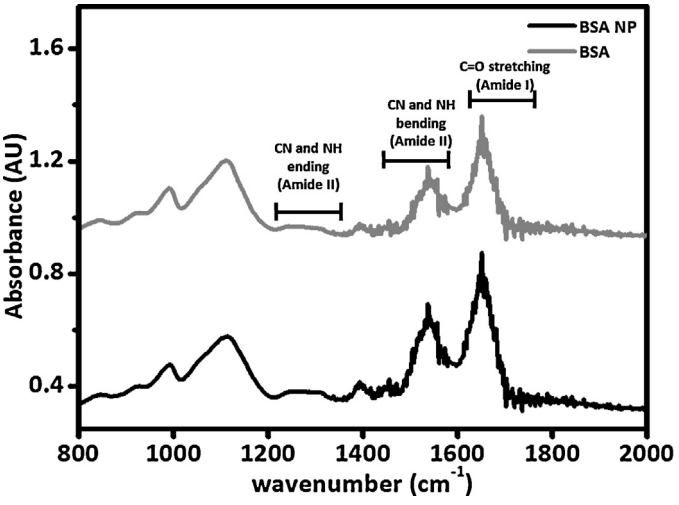

Fig. 11. ATR FT-IR spectra of BSA protein and BSA-NPs corresponding to the amide region.

As an alternative reticulated method, an ethanol solution of BSA was also cross-linked by a chemical cross linker such as glutaraldehyde. NPs of mean diameter similar to that of irradiated ones were obtained (non-statistically different) (Table 1). These data are also in agreement with a sequential mechanism of NP formation.

3.2. Structure-function of BSA-NPs

Merocyanine 540 (MC540) is a negatively charged anti-tumor photosensitizer, able to interact with BSA with two types of complexes, 1:1 and 2:1, according to the MC540/protein ratios [37]. In this work, the fluorescence signal from aromatic amino acids were used to study the interaction with MC540 [38]. No shifts of the FTIR spectra were observed for BSA or BSA-NPs (data not shown).

The data of fluorescence studies plotted in Fig. 12 allow understanding the interaction of BSA and BSA-NPs with MC540. The BSA protein has two main hydrophobic pockets for drug binding called Sudlow sites I and II. Sudlow site I contains Trp212, while Sudlow site II is governed mainly by tyrosines [18,37].

Trp alone (λ_{ex} = 295 nm) or both Trp and Tyr (λ_{ex} = 280 nm) can be analyzed by using different excitation wavelengths. Fig. 12 shows that BSA-NPs have near half of the emission intensity of BSA. This could be explained as the NPs have internal quenching as a consequence of a closer distance of Trp from different BSA molecules. An alternative explanation is that certain Trp could have been damaged during irradiation of the sample for NP formation. However, the latter is not feasible as the UV–vis analysis done previously showed no changes in such amino acid absorption. In addition, previous studies have demonstrated the existence of internal quenching during the nanostructuration process using fluorescein-labeled BSA [16].

The presence of MC540 quenches the emission fluorescence of the aromatic amino acids (Trp and Tyr) while interacting with the hydrophobic pockets of the protein or NPs. Considering that only few of the 27 Tyr available in the BSA molecule could interact with MC540 through Sudlow site II, the excitation wavelength at 280 nm will show small changes. In contrast, the excitation wavelength at 295 nm, which corresponds to only two Trp, will be more sensitive to the interaction with MC450. Therefore, we analyzed this last excitation condition.

The contribution of the quenching by the probe can be analyzed using a relative fluorescence ratio (Fig. 12 (c) and (d)). These data allowed calculating the affinity parameters K_d and B_{max} through Scatchard analysis (Table 2). BSA-NPs showed around half of the binding sites compared to BSA protein (Fig. 12 and Table 2). This could be explained by the fact that, in each NP, several BSA molecules are completely hidden and not available to interact with MC540 in the solution. The affinity interaction of the NPs was similar than that of the monomeric protein, as described by the dissociation constant.

An experiment was made in which a solution of MC540 (45 μM) was incubated with the same amount of BSA or BSA-NP solutions (45 μM) for different length of time. Then, free MC540 was separated using a membrane device (Vivaspin 500, 3 kDa MWCO). The amount of drug bound to the vehicle was quantified by UV–vis spectroscopy using a Nano-drop 1000 spectrophotometer. The results of the binding efficiency are displayed in the Table 3. After 60 min the 100% of binding efficiency is reached with BSA. In case of the BSA-NP the efficiency of 75% is reached after 20 min.

The kinetic release profile assays performed using MC540-loaded samples showed that despite the slightly lower efficiency in binding the drug (BSA-NPs 77% vs BSA 99% after a releasing time of 40 min), the NPs showed no drastic differences when compared to the kinetic release profile of BSA (Fig. 13). The Michaelis-Menten fitting of the releasing curves also showed that the protein had a smaller K_M (4.9 ± 2.5) than the BSA-NPs (9.0 ± 3.2).

The results obtained not only support the structure-function similarity of BSA and BSA-NPs, but also show that BSA-NPs are comparable to BSA and that the functionality of the protein is preserved. Independently of the small differences in the binding affinity, we may consider that the NPs are able to interact and deliver other therapeutic drugs such as Emodin or Uracil.

3.3. NP preparation with other proteins

Lysozyme (Lyso) was chosen as a second model protein to prepare NPs. Lyso is a commercial bacteriolytic enzyme with antimicrobial activity against Gram + bacteria, which is very sensitive to very low ethanol concentrations. As shown in Fig. 14, large particles (mean diameter in the range of 400–900 nm) were found in the Lyso solutions when ethanol was added. Therefore, it was not possible to prepare stable Lyso NPs.

In aqueous ethanol solution, as ethanol concentration rises, Lyso exists successively as a monomer, dimer, protofilament and amyloid fibrils states [39]. Small amount of ethanol (5% v/v) shows changes of the Lyso–Lyso interaction [40]. It has been reported that in the ethanol concentration range from 0 to 63% (v/v) there is a strong repulsion between macromolecules in systems prepared from purified Lyso and deionized water. This behavior is interpreted in terms of adsorption of alcohol molecules on hydrophobic sites found onto the protein surface, reducing the attractive hydrophobic forces (and therefore increasing the solubility). However, the addition of a very small amount of salt (or buffer), in the range of 1–10 mM, can cause instantaneous turbidness of the solution and also a rapid gel formation when ethanol concentration is high [41].

As an alternative method to prepare Lyso-NPs, we used three different BSA/Lyso molar ratios in buffer containing 35% ethanol. Fig. 15 shows the plot of the mean diameter of the protein solutions

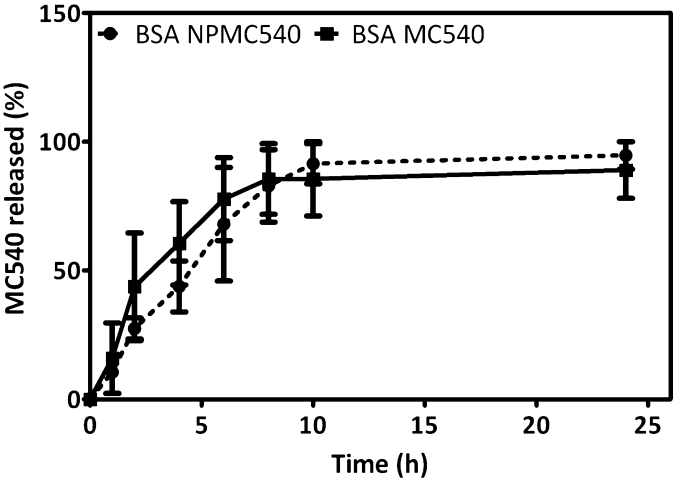

Fig. 13. Releasing profile of MC540 from BSA and BSA-NPs loaded with the probe.

Table 3
Binding efficiency at different incubation times.

Sample	Incubation time (min)	Binding efficiency (%)
BSA MC540	0	51 ± 36
	20	74 ± 12
	40	99 ± 17
	60	100 ± 9
BSA NP MC540	0	43 ± 5
	20	75 ± 11
	40	77 ± 5
	60	73 ± 10

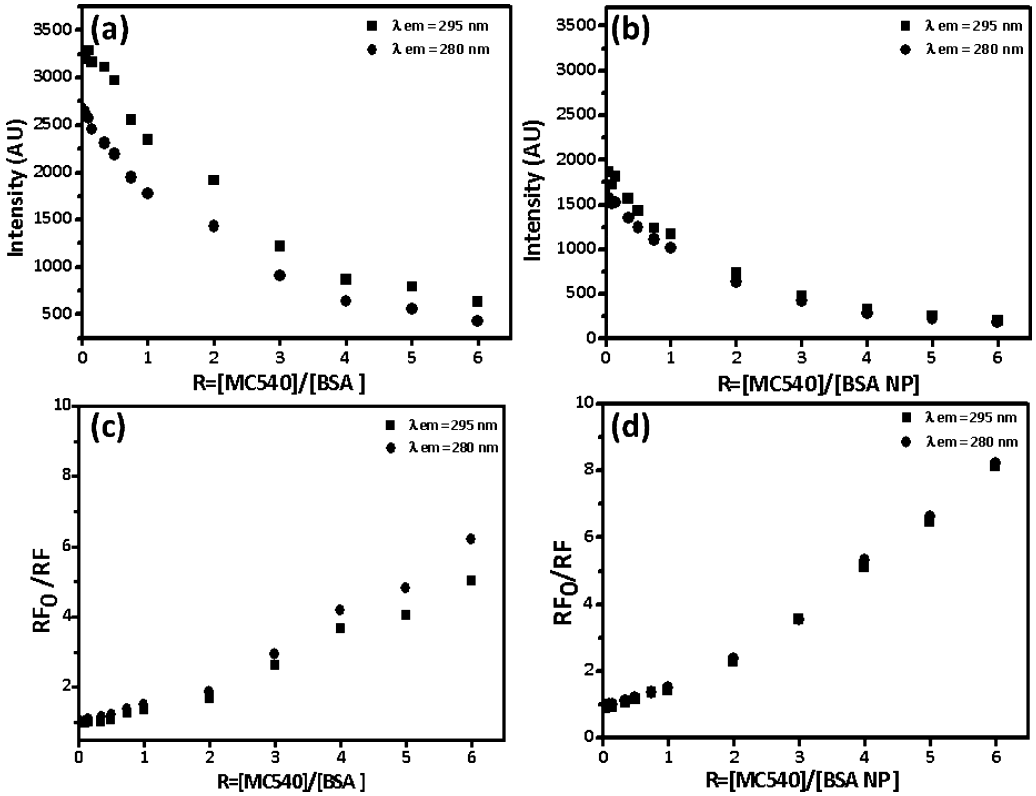

Fig. 12. Plots of fluorescence emission at different (a) MC540/BSA and (c) MC540/BSA-NP ratios. Plots of relative fluorescence emission at different MC540/BSA and MC540/BSA-NP ratios are shown in (b) and (d) respectively.

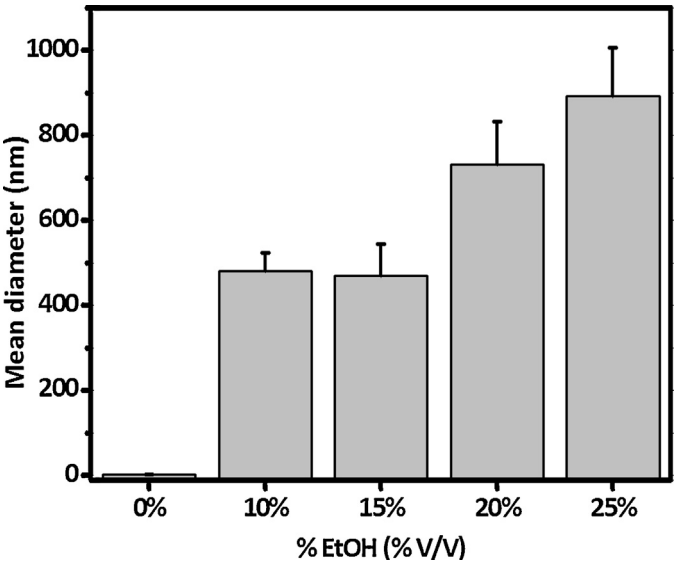

Fig. 14. Plot of mean diameter of Lysozyme solution containing different amounts of ethanol.

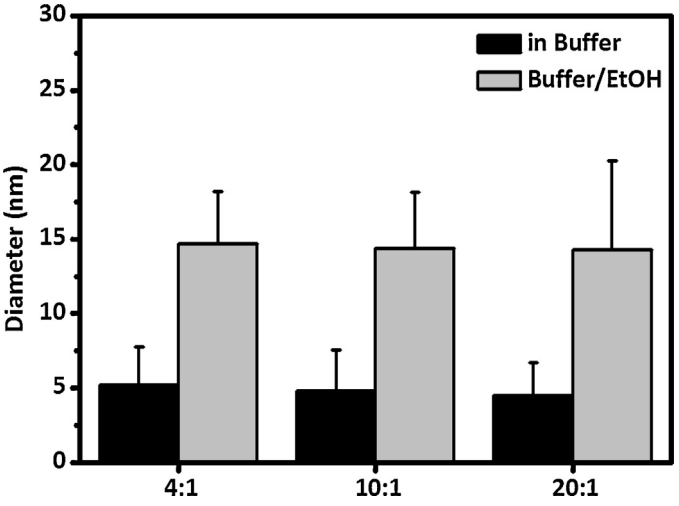

Fig. 15. Mean diameter in ethanol solution BSA/Lyso prepared in different molar ratios.

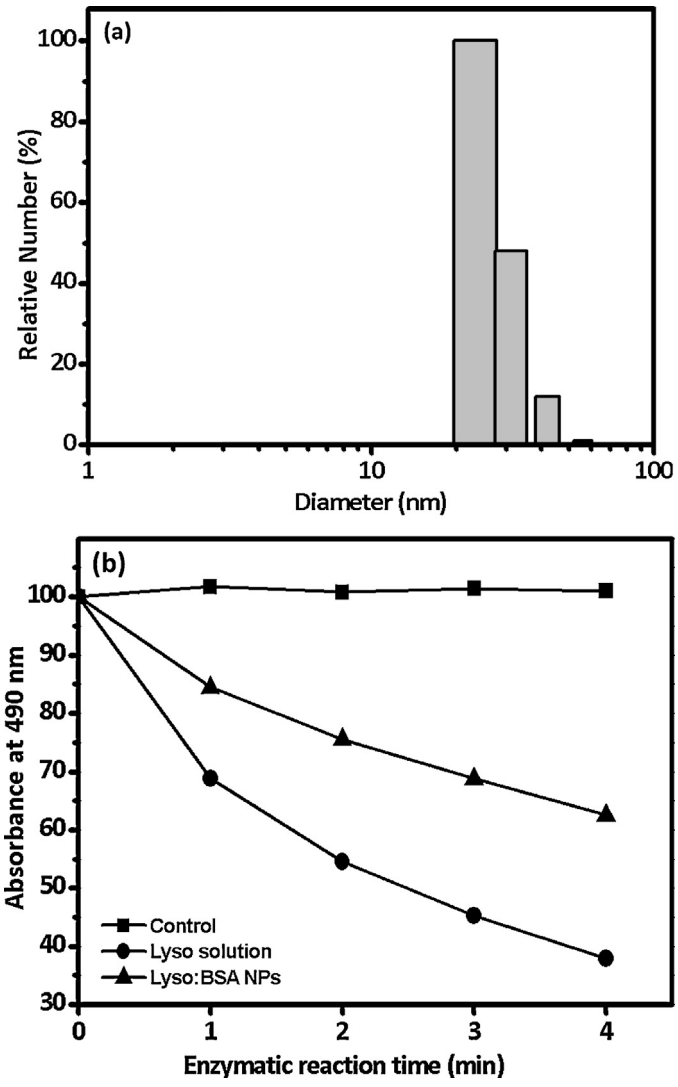

Fig. 16. (a) Plots of particle diameter distribution of BSA/Lyso (20:1) after irradiation; (b) plot of turbidity of *Micrococcus lysodeikticus* suspension (enzymatic activity) after addition of the enzyme or BSA/Lyso NPs.

in buffer containing ethanol before irradiation in a gamma source. The same types of aggregates were observed in all cases.

Considering the possibility of low availability of Lyso, the highest protein ratio (20:1) was selected for irradiation. After 10 kGy irradiation, ethanol was removed from the sample by size exclusion chromatography. A further purification step was performed to remove the free protein by successive centrifugation steps.

In all the experimental conditions studied in this report, BSA is the main component of the protein mixture (from 80% to 95% in molar base). In addition, Lyso molecule has more than four-times lower molecular weight than BSA. Therefore, results suggest that the aggregation mechanism is dominated by BSA, and as it is demonstrated in the previous experiments, the BSA aggregation is dependent of ethanol concentration. Thus, it is highly possible the Lyso self-aggregation is inhibited by the high BSA proportion in the mixture and Lyso coaggregates onto BSA macrostructures.

The presence of active Lyso in the BSA/Lyso-NPs was assessed by measuring the bacteriolytic activity against *Micrococcus lysodeikticus*. Fig. 16 shows the DLS histogram and the enzymatic activity plot of BSA-Lys NPs. The lytic activity of the bi-protein NPs showed a trend similar to that of free Lyso.

4. Conclusions

Protein NPs can be prepared by irradiation of protein solutions in water/ethanol mixtures, using ionizing radiation sources. Experimental data support the hypothesis of a two-step process where protein aggregation occurs in the water/solvent mixture before the irradiation process. Different ethanol concentrations reveal the presence of particles of different sizes which can be dynamically interconverted. After irradiation with an ionizing source, an irreversible process of aggregation occurs.

Near and far CD spectra showed different information about the secondary and ternary structure of BSA. Far CD spectra showed a slight reduction in the alpha helix content of the protein secondary structure. UV–vis spectra showed no changes in the aromatic amino acid microenvironments but possible modification of thiol groups are suspected. FT-IR analysis of the partially hydrated samples showed no overall changes in the protein backbone. The results of these studies allow concluding that the BSA molecules that constitute the NPs are mainly in the native conformation. The flu-

orescence properties of the aromatic amino acids of BSA and the use of a chemical probe can allow demonstrating the functionality of the BSA-NPs. Small changes in the adsorption and desorption properties were measured in the NPs compared to the seed protein.

Few proteins have the aggregative behavior of BSA in ethanol solutions. However, by mixing BSA with other proteins in the initial solution, it is possible to prepare specific NPs containing a desired property. Here, we prepared bi-protein NPs by mixing Lyso and BSA and demonstrated their functionality. In addition, a low amount of the specific protein is required as the BSA is the main NP component. We envision that highly specific protein NPs can be prepared by this technique by selecting the appropriate protein to be mixed with BSA.

Acknowledgements

E.A. and C.F. thank ANPCyT for the fellowship. S.A. and M.G. are researchers from CONICET. This work was partially supported by grants from Universidad Nacional de Quilmes (Buenos Aires, Argentina), IAEA and MINCyT (Argentina), and National Science Centre Poland UMO-2012/07/B/ST4/01429.

References

[1] M. Ulbricht, Advanced functional polymer membranes, Polymer 47 (2006) 2217–2262.
[2] A.M. Ventura, H.M.F. Lahore, E.E. Smolko, M. Grasselli, High-speed protein purification by adsorptive cation-exchange hollow-fiber cartridges, J. Membr. Sci. 321 (2008) 350–355.
[3] J. Peters Jr., A.J. Stewart, Albumin research in the 21st century, Biochimica et Biophysica Acta (BBA) – General Subjects 1830 (2013) 5351–5353.
[4] B. Elsadek, F. Kratz, Impact of albumin on drug delivery—New applications on the horizon, J. Control. Rel. 157 (2012) 4–28.
[5] T. Peters, All About Albumin: Biochemistry Genetics, and Medical Applications, Elsevier Science, 1995.
[6] G. Fanali, A. di Masi, V. Trezza, M. Marino, M. Fasano, P. Ascenzi, Human serum albumin: from bench to bedside, Mol. Aspects Med. 33 (2012) 209–290.
[7] H.-H. Chao, D.F. Torchiana, BioGlue: albumin/glutaraldehyde sealant in cardiac surgery, J. Card. Surg. 18 (2003) 500–503.
[8] A.O. Elzoghby, W.M. Samy, N.A. Elgindy, Albumin-based nanoparticles as potential controlled release drug delivery systems, J. Control. Release 157 (2012) 168–182.
[9] C. Weber, C. Coester, J. Kreuter, K. Langer, Desolvation process and surface characterisation of protein nanoparticles, Int. J. Pharm. 194 (2000) 91–102.
[10] S.H. Lee, D. Heng, W.K. Ng, H.-K. Chan, R.B.H. Tan, Nano spray drying: a novel method for preparing protein nanoparticles for protein therapy, Int. J. Pharm. 403 (2011) 192–200.
[11] N. Desai, Nanoparticle albumin bound (nab) technology: targeting tumors through the endothelial gp60 receptor and SPARC, Nanomed. Nanotechnol. Biol. Med. 3 (2007) 339.
[12] J. Cortes, C. Saura, Nanoparticle albumin-bound (nab™)-paclitaxel: improving efficacy and tolerability by targeted drug delivery in metastatic breast cancer, EJC Supplements 8 (2010) 1–10.
[13] R. Xu, M. Fisher, R.L. Juliano, Targeted albumin-based nanoparticles for delivery of amphipathic drugs, Bioconjug. Chem. 22 (2011) 870–878.
[14] J. Gong, M. Huo, J. Zhou, Y. Zhang, X. Peng, D. Yu, H. Zhang, J. Li, Synthesis, characterization, drug-loading capacity and safety of novel octyl modified serum albumin micelles, Int. J. Pharm. 376 (2009) 161–168.
[15] S.M. Vaiana, A. Emanuele, M.B. Palma-Vittorelli, M.U. Palma, Irreversible formation of intermediate BSA oligomers requires and induces conformational changes, Proteins: Struct. Funct. Bioinform. 55 (2004) 1053–1062.
[16] S.L. Soto Espinoza, M.L. Sánchez, V. Risso, E.E. Smolko, M. Grasselli, Radiation synthesis of seroalbumin nanoparticles, Radiat. Phys. Chem. 81 (2012) 1417–1421.
[17] G.H.C. Varca, C.C. Ferraz, P.S. Lopes, M. Mathor, b, M. Grasselli, A.B. Lugão, Radio-synthesized protein-based nanoparticles for biomedical purposes, Radiat. Phys. Chem. 94 (2014) 181–185.
[18] P. Sevilla, J.M. Rivas, F. García-Blanco, J.V. García-Ramos, S. Sánchez-Cortés, Identification of the antitumoral drug emodin binding sites in bovine serum albumin by spectroscopic methods, Biochim. et Biophys. Acta (BBA) – Proteins Proteomics 1774 (2007) 1359–1369.
[19] M.G. Wacker, Nanotherapeutics—product development along the nanomaterial discussion, J. Pharm. Sci. 103 (2014) 777–784.
[20] M.S. Sachdeva, Drug targeting systems for cancer chemotherapy, Expert Opin. Investig. Drugs 7 (1998) 1849–1864.
[21] Patwekar, S., Gattani, S., Giri, R., Bade, A., Sangewar, B., Raut, V., REVIEW ON NANOPARTICLES USED IN COSMETICS AND DERMAL PRODUCTS, 2014.
[22] J.J. Marty, R.C. Oppenheim, P. Speiser, Nanoparticles–a new colloidal drug delivery system, Pharm. Acta Helv. 53 (1978) 17–23.
[23] E.J. Cohn, W.L. Hughes, J.H. Weare, Preparation and properties of serum and plasma proteins. XIII. Crystallization of serum albumins from ethanol–water mixtures[1a,b], J. Am. Chem. Soc. 69 (1947) 1753–1761.
[24] C.J. van Oss, On the mechanism of the cold ethanol precipitation method of plasma protein fractionation, J. Protein Chem. 8 (1989) 661–668.
[25] P. Ulański, S. Kadłubowski, J.M. Rosiak, Synthesis of poly (acrylic acid) nanogels by preparative pulse radiolysis, Radiat. Phys. Chem. 63 (2002) 533–537.
[26] S. Kadlubowski, J. Grobelny, W. Olejniczak, M. Cichomski, P. Ulanski, Pulses of fast electrons as a tool to synthesize poly(acrylic acid) nanogels. intramolecular cross-linking of linear polymer chains in additive-free aqueous solution, Macromolecules 36 (2003) 2484–2492.
[27] S. Kadlubowski, P. Ulanski, J.M. Rosiak, Synthesis of tailored nanogels by means of two-stage irradiation, Polymer 53 (2012) 1985–1991.
[28] S. Kadlubowski, Radiation-induced synthesis of nanogels based on poly(*N*-vinyl-2-pyrrolidone)—a review, Radiat. Phys. Chem. 102 (2014) 29–39.
[29] P. Ulański, I. Janik, J.M. Rosiak, Radiation formation of polymeric nanogels, Radiat. Phys. Chem. 52 (1998) 289–294.
[30] P. Ulanski, J.M. Rosiak, The use of radiation technique in the synthesis of polymeric nanogels, Nucl. Instrum. Methods Phys. Res. Sect. B 151 (1999) 356–360.
[31] J.-C. An, A. Weaver, B. Kim, A. Barkatt, D. Poster, W.N. Vreeland, J. Silverman, M. Al-Sheikhly, Radiation-induced synthesis of poly(vinylpyrrolidone) nanogel, Polymer 52 (2011) 5746–5755.
[32] C. Dispenza, N. Grimaldi, M.A. Sabatino, S. Todaro, D. Bulone, D. Giacomazza, G. Przybytniak, S. Alessi, G. Spadaro, Studies of network organization and dynamics of e-beam crosslinked PVPs: from macro to nano, Radiat. Phys. Chem. 81 (2012) 1349–1353.
[33] T. Schmidt, I. Janik, S. Kadłubowski, P. Ulański, J.M. Rosiak, R. Reichelt, K.-F. Arndt, Pulsed electron beam irradiation of dilute aqueous poly(vinyl methyl ether) solutions, Polymer 46 (2005) 9908–9918.
[34] K. Furusawa, K. Terao, N. Nagasawa, F. Yoshii, K. Kubota, T. Dobashi, Nanometer-sized gelatin particles prepared by means of gamma-ray irradiation, Colloid Polym. Sci. 283 (2004) 229–233.
[35] Y. Akiyama, T. Fujiwara, S.-I. Takeda, Y. Izumi, S. Nishijima, Preparation of stimuli-responsive protein nanogel by quantum-ray irradiation, Colloid Polym. Sci. 285 (2007) 801–807.
[36] J. Grdadolnik, Y. Marechal, Bovine serum albumin observed by infrared spectrometry. I. Methodology, structural investigation, and water uptake, Biopolymers 62 (2001) 40–53.
[37] M. Banerjee, U. Pal, A. Subudhhi, A. Chakrabarti, S. Basu, Interaction of Merocyanine 540 with serum albumins: photophysical and binding studies, J. Photochem. Photobiol. B: Biol. 108 (2012) 23–33.
[38] F.W.J. Teale, G. Weber, Ultraviolet fluorescence of the aromatic amino acids, Biochem. J. 65 (1957) 476–482.
[39] Y. Yonezawa, S. Tanaka, T. Kubota, K. Wakabayashi, K. Yutani, S. Fujiwara, An Insight into the Pathway of the amyloid fibril formation of hen egg white lysozyme obtained from a small-angle X-ray and neutron scattering study, J. Mol. Biol. 323 (2002) 237–251.
[40] W. Liu, D. Bratko, J.M. Prausnitz, H.W. Blanch, Effect of alcohols on aqueous lysozyme–lysozyme interactions from static light-scattering measurements, Biophys. Chem. 107 (2004) 289–298.
[41] S. Tanaka, Y. Oda, M. Ataka, K. Onuma, S. Fujiwara, Y. Yonezawa, Denaturation and aggregation of hen egg lysozyme in aqueous ethanol solution studied by dynamic light scattering, Biopolymers 59 (2001) 370–379.